Resonant Frequency Selectable Induction Heating Targets

John I. Rodriguez Steven B. Leeb
Laboratory for Electromagnetic and Electronic Systems
Massachusetts Institute of Technology
Cambridge, MA 02139, USA

***Abstract*— This paper examines a scheme for developing frequency selectable induction heating targets for stimulating temperature sensitive polymer actuators. "Frequency selectable" implies that each target has a frequency at which it heats preferentially compared to other remaining targets. Resonant RLC circuits that are inductively coupled to a primary induction coil are examined. One way to achieve selectivity with frequency is to design each target to have a different resonant frequency. In this way, a target driven at its resonant frequency will heat preferentially when compared to the remaining targets.**

I. Background

A dynamic vibration absorber (DVA) is an auxiliary spring-mass system that is coupled to a vibrating structure [1]. Typically, a DVA is designed to provide maximum damping at a fixed natural frequency. A more sophisticated DVA can adjust its natural frequency by varying its spring constant with a magnetic actuator, a shape-memory alloy, or some other mechanical scheme [2]. Because the DVA concept applies equally well to both linear and rotational systems, we are exploring an additional approach: a DVA which can adjust its natural frequency by controlling its moment of inertia. A variable inertia can be made from a cylindrical container filled with a variable viscosity fluid. This fluid can be created using a solution of temperature sensitive polymer gel beads suspended in a solvent [3]. Below a certain temperature the gel beads swell, absorbing the surrounding solvent into the polymer matrix (like a sponge). When this happens the gel beads pack tightly in the container, adding significantly to the container's moment of inertia. At higher temperatures the polymer network shrinks, allowing the solvent to flow freely. This effectively decouples the gel-solvent mass and lowers the apparent rotational inertia. By subdividing the container into n compartments of varying gel mass, 2^n anti-resonant states are made possible depending on which compartments are heated.

By design, each gel compartment is hermetically sealed and allowed to oscillate mechanically with as little external damping as possible. Heating schemes that need to make contact with a gel compartment are therefore undesirable. Induction heating can be used to trigger the gel in each compartment without physical contact [4]. The induction heating system must be capable of selectively heating any combination of gel compartments. One approach to achieve this goal outfits each gel compartment with an induction target that has been designed to heat preferentially at one frequency (with respect to the other targets). In this case, a single power supply that can impress a sum-of-sinewaves in voltage across a single induction coil could heat the desired combination of inductively coupled targets. This approach does not require a separate induction coil for each target, unlike other multi-load/single-converter induction heating systems [5].

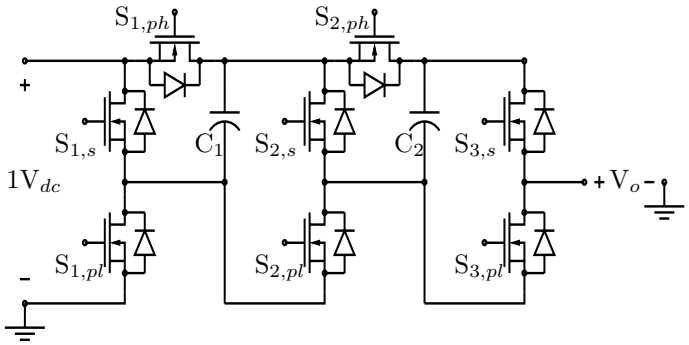

Fig. 1. A four-level Marx inverter.

A Marx multilevel inverter topology is used to approximate the desired sum-of-sinewaves voltage [6]-[8]. This multilevel inverter is capable of simultaneous power delivery at multiple frequencies and is the subject of a separate paper [6]. For illustration, one phase leg of a four-level Marx inverter is shown in Fig. 1. Using two phase legs an induction coil can be driven differentially with a sum-of-sinewaves voltage waveform. The scope plot for a sample drive consisting of sinewaves at 25KHz and 50KHz is provided in Fig. 2. Three waveforms are shown in total: the desired reference waveform, its multilevel "staircase" approximation, and the current supplied to the induction heating coil (shown bottom).

II. Resonant, Frequency Selectable Induction Heating Targets

Two types of frequency selectable induction targets could be employed: nonresonant and resonant. The first approach consists of inductively-coupled RL circuits, where selective heating is achieved by varying the re-

0-7803-8269-2/04/$17.00 (C) 2004 IEEE.

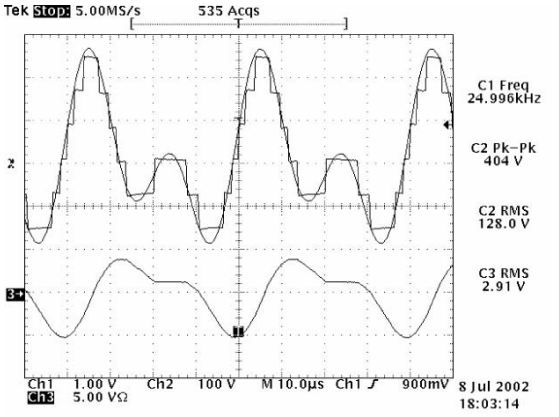

Fig. 2. The Marx inverter "staircase" approximation of a sum-of-sinewaves at 25KHz and 50KHz.

sistance of the targets [7]. The latter involves making a collection of resonant RLC circuits, each inductively coupled to a primary heating coil. In this case, the target's capacitance is chosen so that the effective series resistance in the circuit dissipates power preferentially at the circuit's resonant frequency. When compared to the RL scheme, the RLC target allows for a greater degree of preferential heating while keeping the required target frequencies in a tighter frequency band. The primary coil used to excite these targets can be driven with either a current or voltage source. Both drive conditions and their implications are considered.

A. Induction Heating: Current Drive Case

The design of a multiple resonant induction target system can be a challenge because of the large number of parameters to be specified. A designer must simultaneously balance geometry, thermal issues, and the selection of several components all while trying to achieve a desired degree of "selectivity" in an acceptable frequency band. To make matters worse, these systems have the potential to be coupled to such an extent that a target can not be designed without taking into account its affect on the remaining targets. A designer is then forced to evaluate the design using a computer, a method that provides little insight for improvement. Fortunately, some insight can be had from examining cases that are not highly coupled.

Consider the situation where only one resonant circuit exists ($n = 1$) as indicated in Fig. 3 by R_n, L_n, and C_n. This network is coupled to a primary induction coil, L_0, which is driven by the sinusoidal current, $I_0 = I_o sin(\omega t)$.

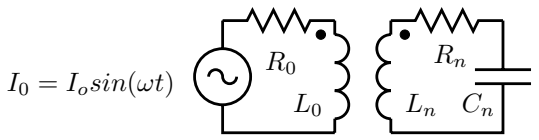

Fig. 3. Induction heating circuit for one resonant target, in this case the primary coil is driven by a sinusoidal current source.

If we denote the mutual inductance between coil L_0 and L_n as L_{0n}, the coupling coefficient between the two coils, K_n, is defined as

$$K_n = \frac{L_{0n}}{\sqrt{L_0 L_n}}. \tag{1}$$

The time averaged power dissipated in R_n can then be expressed as

$$\langle P_n(\omega)\rangle = \frac{(I_o K_n \omega^2)^2 L_0 L_n R_n}{2[(1 - L_n C_n \omega^2)^2 + (R_n C_n \omega)^2]}. \tag{2}$$

Maximum power is delivered at the natural frequency,

$$\omega_n = \frac{1}{\sqrt{L_n C_n}}, \tag{3}$$

which simplifies (2) to the following:

$$\langle P_n(\omega_n)\rangle = \frac{(I_o K_n \omega_n)^2 L_0 L_n}{2R_n} = \frac{(I_o K_n)^2 L_0}{2R_n C_n} \tag{4}$$

Alternatively, (4) can be expressed in terms of target n's "quality" factor,

$$Q_n = \frac{L_n \omega_n}{R_n}, \tag{5}$$

to give

$$\langle P_n(Q_n)\rangle = \frac{(I_o Q_n K_n)^2 R_n}{2}. \tag{6}$$

Consequently, the power dissipated in a target is commensurate with its Q. For the current drive case these relationships will hold equally well for multiple simultaneous targets providing that there is no cross-coupling between targets, i.e. any mutual inductance between target coils is identically zero. When at least two targets are present, it is useful to know the frequencies that lead to the greatest amount of preferential heating. The degree of heating in a target n compared to a target m can be expressed as

$$\frac{\langle P_n(\omega)\rangle}{\langle P_m(\omega)\rangle} = \frac{K_n^2 L_n R_n[(1 - L_m C_m \omega^2)^2 + (R_m C_m \omega)^2]}{K_m^2 L_m R_m[(1 - L_n C_n \omega^2)^2 + (R_n C_n \omega)^2]}. \tag{7}$$

The desired frequencies can be found by taking the derivative of (7) and setting it equal to zero

$$\frac{d}{d\omega}\left(\frac{\langle P_n(\omega)\rangle}{\langle P_m(\omega)\rangle}\right) = 0. \tag{8}$$

This leads to a fifth order polynomial in ω,

$$a\omega^5 + b\omega^3 + c\omega = 0 \tag{9}$$

where the coefficients are as follows:

$$\begin{aligned} a =& [(R_n C_n)^2 - 2L_n C_n](L_m C_m)^2 - \\ & [(R_m C_m)^2 - 2L_m C_m](L_n C_n)^2 \\ b =& [2(L_m C_m)^2 - 2(L_n C_n)^2] \\ c =& [(R_m C_m)^2 - 2L_m C_m] - [(R_n C_n)^2 - 2L_n C_n]. \end{aligned} \tag{10}$$

Only two of the polynomial's roots are relevant as one of the roots is zero and the other two are negative. The valid roots are

$$\omega = \sqrt{\frac{-b \pm \sqrt{b^2 - 4ac}}{2a}}. \tag{11}$$

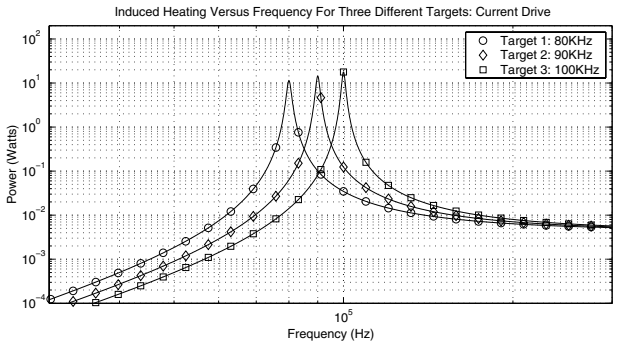

(a) Power profiles for 3 different targets.

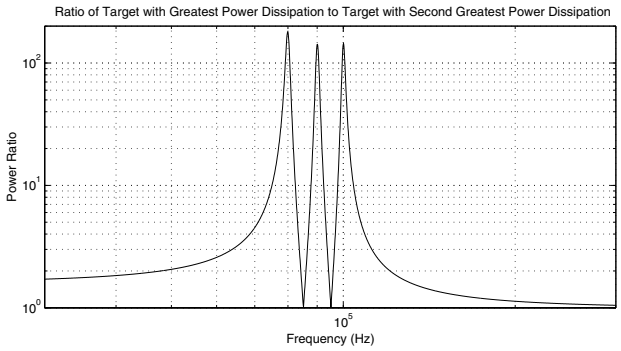

(b) Ratio of delivered power between targets.

Fig. 4. Induction heating power curves versus frequency for 3 different targets assuming a current source drive of $I_o = 1A$.

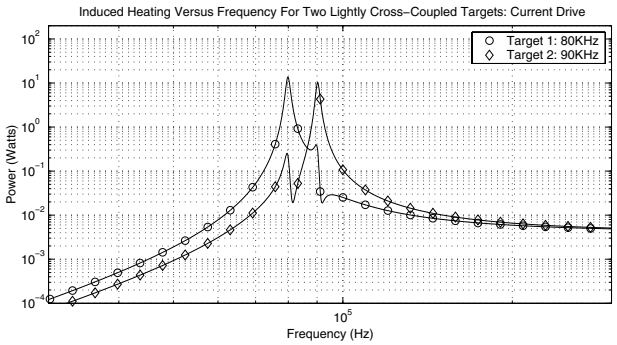

(a) Power profiles for 2 different targets.

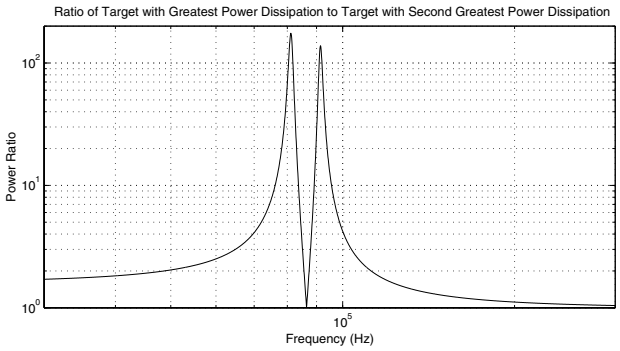

(b) Ratio of delivered power between targets.

Fig. 5. Induction heating power curves versus frequency for 2 different targets assuming a current source drive of $I_o = 1A$.

If the Q's of the resonant targets are high enough, the solution to (11) will equal the natural frequencies of the two targets to a close approximation. Equation (4) makes apparent that for a fixed current the absolute power delivered to a target will vary depending on the target's component values. In order to equalize the absolute power delivered to all targets the amplitude of the current driving the primary coil can be controlled via the following relationship:

$$I_0(\omega_{n+1}) = \frac{K_n}{K_{n+1}}\sqrt{\frac{R_{n+1}C_{n+1}}{R_nC_n}}I_0(\omega_n). \qquad (12)$$

These results are easier to understand by examining the time averaged power versus frequency for three hypothetical targets shown in Fig. 4 (a). In this example the primary coil, $L_0 = 10\mu H$, and there are three target coils (n=1,2,3), $L_n = 100\mu H$. Likewise their resistances are given by $R_n = 1\Omega$. The resistance of the primary coil is also $R_0 = 1\Omega$ but irrelevant because of the current source drive. The coupling coefficient of all targets has been arbitrarily set to 0.3 and the capacitances, C_n of the three targets ($n = 1, 2, 3$) have been chosen to give natural frequencies at 80KHz, 90KHz, and 100KHz. With these constraints each target experiences preferential heating with respect to the remaining targets over some frequency range. The extent of preferential heating is given as a ratio in Fig. 4 (b) and clearly exceeds 100 near the natural frequencies of the targets in this example.

So far only targets with negligible cross-coupling have been considered. In reality, mutual inductance always exists between targets and cannot always be ignored. Even a small degree of cross-coupling can have a noticeable effect on the power profile of a target. The inclusion of cross-coupling terms lead to increasingly complicated transfer function descriptions of the system without much additional insight. Instead of looking at the transfer functions in detail, consider the impact of cross-coupling on the hypothetical targets discussed earlier. For simplicity target 3 has been removed and targets 1 and 2 now have a cross-coupling coefficient of 0.03, a number which is ten times smaller than their respective coupling to the primary coil. For this example the power profiles of the two targets are shown in Fig. 5 (a). Previously, each target exhibited one resonant frequency. Now each target experiences an additional resonance located close to the natural frequency of the target it is cross-coupled to, as well as an anti-resonance to the right of this "new resonant frequency." Fig. 5 (b) shows the ratio of heating between targets. From this figure it is apparent that the frequencies where the ratio is maximized are now higher, corresponding more closely to the location of the anti-resonant frequencies.

B. Induction Heating: Voltage Drive Case

The current drive case is insightful because it makes apparent the excitation frequencies that give the greatest degree of preferential heating. The Marx inverter naturally

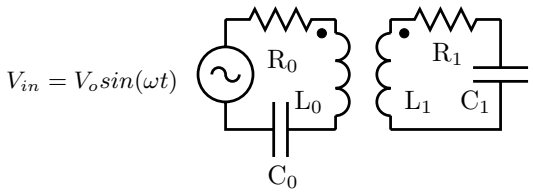

Fig. 6. Induction heating circuit for 1 resonant target, in this case the primary coil is driven by a sinusoidal voltage source.

applies a voltage at its output and supplies current as determined by the driving point impedance. If the impedance looking into the primary coil is known, the current drawn from the converter can be calculated and the equations from the previous section applied.

Consider Fig. 6 which represents the induction heating circuit from before with some minor changes. The current source has been replaced with a voltage source and as a practical matter, a dc blocking capacitor C_0, has been inserted on the source side. If only one target is present, the expression for the load impedance $Z_{load}(s)$ is a rational transfer function of the form:

$$Z_{load}(s) = \frac{Z_n(s)}{Z_d(s)}, \tag{13}$$

where the numerator is

$$Z_n(s) = (L_0 s + R_0 + \frac{1}{C_0 s})(L_1 s + R_1 + \frac{1}{C_1 s}) - (L_{01} s)^2, \tag{14}$$

and the denominator is

$$Z_d(s) = (L_1 s + R_1 + \frac{1}{C_1 s}). \tag{15}$$

If the impedances associated with R_0 and C_0 are small at the frequencies of interest (typical of a practical design), then (13) can be simplified to

$$Z_{load}(s) = \frac{L_0 s[L_1(1 - K_1^2)C_1 s^2 + R_1 C_1 s + 1]}{L_1 C_1 s^2 + R_1 C_1 s + 1}. \tag{16}$$

From (16) it can be inferred that the load impedance will experience a maximum near the natural frequency of the target,

$$\omega_{Zmax} = \omega_1 = \frac{1}{\sqrt{L_1 C_1}}, \tag{17}$$

and a minimum near

$$\omega_{Zmin} = \frac{1}{\sqrt{L_1 C_1 (1 - K_1^2)}}. \tag{18}$$

This suggests that, for multiple resonant targets (with negligible cross-coupling), the load impedance will experience a local maxima at the natural frequency of each coupled target. The frequencies that lead to the greatest preferential heating can therefore be determined by examining where the load impedance experiences these local maxima.

When more than one target is present and/or the impact of cross-coupled inductors must be taken into account, the

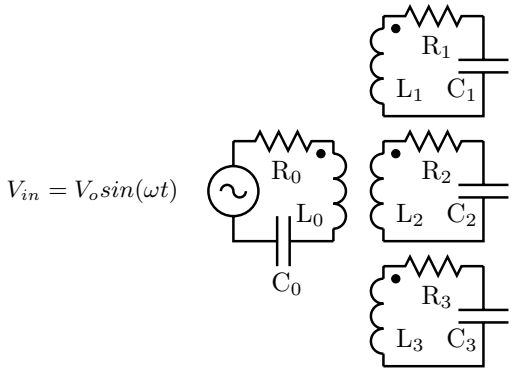

Fig. 7. Induction heating circuit for 3 different targets, in this case the primary coil is driven by a sinusoidal voltage source.

system shown in Fig. 7 can be analyzed using the following compact state-space formulation,

$$\begin{bmatrix} \dot{I} \\ \dot{V} \end{bmatrix} = \begin{bmatrix} -L^{-1}R & L^{-1} \\ -C^{-1} & 0 \end{bmatrix} \begin{bmatrix} I \\ V \end{bmatrix} + \begin{bmatrix} L^{-1} & 0 \\ 0 & 0 \end{bmatrix} \begin{bmatrix} V_{in} \\ 0 \end{bmatrix}, \tag{19}$$

where V_{in} is the input voltage and L is the general inductance matrix of the system, which for the three target case takes the following form:

$$L = \begin{vmatrix} L_0 & L_{01} & L_{02} & L_{03} \\ L_{10} & L_1 & L_{12} & L_{13} \\ L_{20} & L_{21} & L_2 & L_{23} \\ L_{30} & L_{31} & L_{32} & L_3 \end{vmatrix}. \tag{20}$$

Likewise, the resistance and capacitance matrices R and C for the three target network in Fig. 7 can be expressed as

$$R = \begin{vmatrix} R_0 & 0 & 0 & 0 \\ 0 & R_1 & 0 & 0 \\ 0 & 0 & R_2 & 0 \\ 0 & 0 & 0 & R_3 \end{vmatrix}, \tag{21}$$

and

$$C = \begin{vmatrix} C_0 & 0 & 0 & 0 \\ 0 & C_1 & 0 & 0 \\ 0 & 0 & C_2 & 0 \\ 0 & 0 & 0 & C_3 \end{vmatrix}, \tag{22}$$

respectively.

Using (19), the transfer function from V_{in} to I_n (where I_n denotes the current in conductor n for the hypothetical system described in Fig. 7) was calculated in Matlab and is shown in Fig. 8 (a). This example has identical component values to the hypothetical system that generated Fig. 4 in the current driven case. The only difference is the addition of C_0, the dc blocking capacitor which has been chosen to yield a natural frequency with the primary side coil of 50KHz. If the effective resistance of a target is known and does not vary significantly with frequency, the induction heating profile for that target can be determined from its V_{in}-to-I_n transfer function. For a sinusoidal voltage drive of amplitude V_o, the current flowing in conductor n can

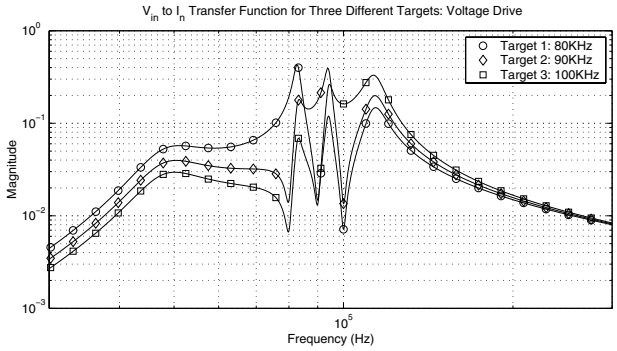

(a) Transfer function for 3 different targets.

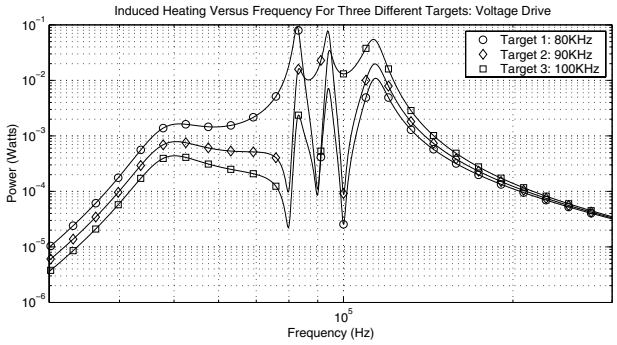

(b) Power profiles for 3 different targets.

Fig. 8. V_{in}-to-I_n transfer function and power curves versus frequency for 3 different targets assuming a voltage drive, V_o=1V.

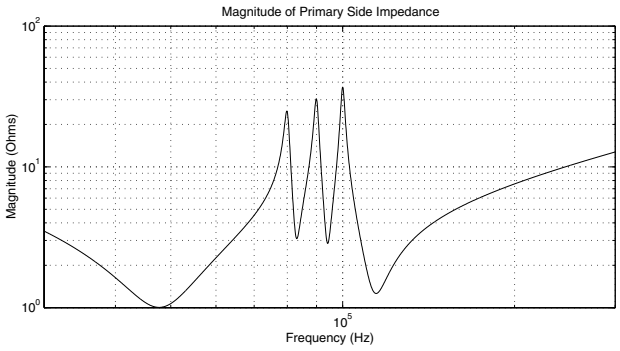

(a) Magnitude of load impedance.

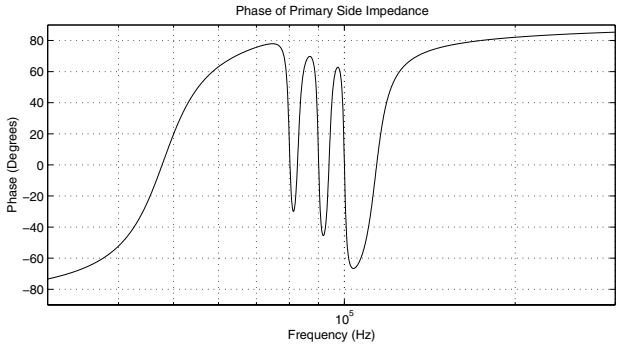

(b) Phase of load impedance.

Fig. 9. Load impedance as seen by converter versus frequency.

be found from Fig. 8 (a) and used to calculate the power dissipated according to the relationship,

$$\langle P_n(\omega)\rangle = \frac{1}{2} I_n(\omega)^2 R_n. \tag{23}$$

Carrying this calculation out, results in the dissipated power curves of each load shown in Fig. 8 (b). In this example the power curves are similar in shape to the magnitude of the transfer function because all of the targets have the same resistance. The voltage source case results in power profiles that are arguably more complicated than the current case. Although the frequencies that give the most preferential heating are unchanged from the current driven case, they no longer maximize the amount of power delivered. As stated previously this can be explained by the variation of the load impedance as a function of frequency. The magnitude and phase of the load impedance for this example are shown in Fig. 9 (a) and (b) respectively. As suggested earlier, the magnitude of the impedance peaks at the frequencies corresponding to the natural frequencies of the various targets. The increased impedance leads to less current drawn and hence a reduction in power. At these frequencies the phase approaches 0^o, so the impedance appears resistive here. The phase also passes through 0^o at frequencies where the power dissipated in a target is maximized. However, the degree of preferential heating is much smaller there.

C. Practical Issues

Resonant RLC induction targets can be constructed in a number of ways. Perhaps the easiest approach is to design each target using a passive element for each of its constituent components, i.e. a separate resistor, inductor and capacitor. For the gel damper application, this approach is less than desirable. Using a lumped resistor as the dissipative element localizes heating to a small area, while consuming precious volume in the gel chamber. A better approach is to rely on the parasitic resistance of the induction coil. If the coil windings are evenly distributed a uniform heating surface can be built. The capacitor could also be eliminated if the self-resonance of the coil is low enough. However, if the inter-winding capacitance of the coil is insufficient, a lumped capacitor must be carefully selected. Because the selectivity of these targets relies on sufficiently high "Q's", it is not uncommon for the winding resistance to be small and the induced current to be high. From a practical standpoint the selected capacitor should have an ESR that is much smaller than the winding resistance. Otherwise, most of the induced heating will occur in the capacitor and not the windings. This is undesirable because the resonant frequency may change significantly with temperature and constant cycling can cause the capacitor to fail. Stable capacitors with low dissipation factors such as silvered mica are ideal for this application, providing the appropriate values are available in reasonable volumes.

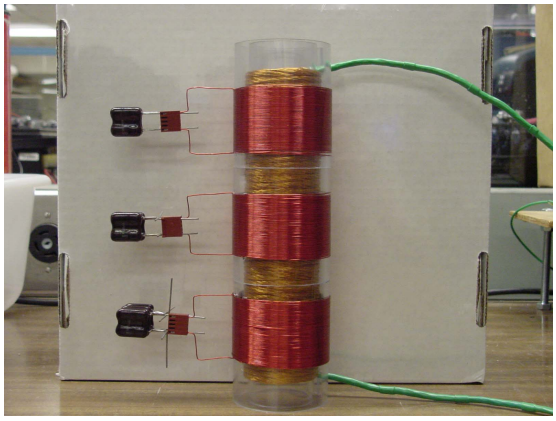

(a) Photo of system

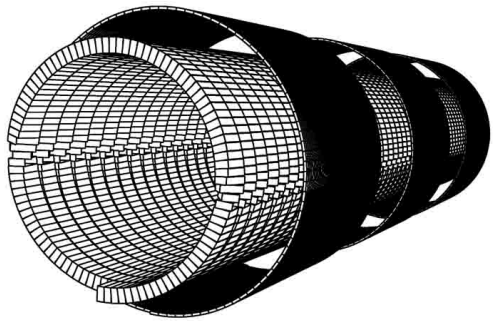

(b) 3-D FastHenry model

Fig. 10. Photo and 3-D model of the multi-resonant induction heating system

D. Experimental Setup: Resonant Targets

A resonant multi-target system was built for testing. The primary coil has a diameter of 4.4cm, a length of 20.4cm and was made from 48 turns of litz wire on a plexiglass former. The three resonant targets have the same 6.32cm diameter with the following lengths: 4.0cm, 4.1cm, 4.2cm. These coils were made from 57, 58, and 59 turns of 22AWG wire, respectively. The output of these targets were paralleled using silvered mica capacitors of the following value: 30nF, 20nF, 40nF. Fig. 10 (a) shows a photo of the primary coil and target coils. In order to calculate the theoretical transfer functions of the system, a 3-D model of each coil was generated and passed to Fasthenry [10] to estimate the inductance matrix for the system. A view of the model used is shown in Fig. 10 (b). The actual transfer functions were then measured for comparison using the test setup shown in Fig. 11. An HP 4395A network analyzer determines the transfer function by sweeping the voltage reference that generates the multilevel sine-wave approximation impressed across the induction coil. The current in each target is then measured via the current probe and amplified before being

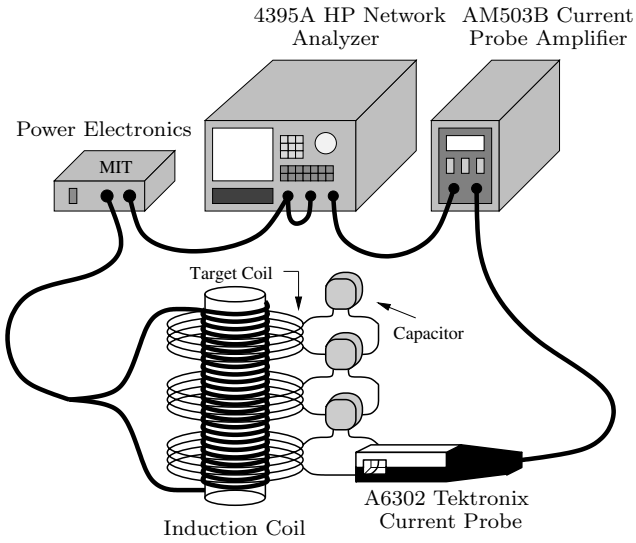

Fig. 11. Multi-wire induction heating experiment.

passed back to the network analyzer. Once all of the V_{in}-to-I_n transfer functions have been characterized, the power profile of each target can be estimated using (23) as discussed previously.

E. Results: Resonant Targets

The measured results from the network analyzer are plotted against a theoretical prediction in Fig. 12. It is clear from the figure that most of the salient features are in agreement. Notably the location of all resonances and anti-resonances are within a few percent of their predicted locations. In general the magnitude of the measured resonances and anti-resonances agree at low frequencies. However there is a growing error with increasing frequency. The reason for this discrepancy can be attributed to the additional ac losses in the windings as a result of skin and proximity effects at higher frequencies. These losses cause the measured maxima and minima to appear more damped than predicted. For this particular fit, the ac resistance of the windings were measured at the low frequency resonances and used to re-estimate the transfer functions. When this resistance is measured for a higher frequency resonance, the fit improves [8].

III. Conclusion

Frequency selectable induction heating targets can be constructed using resonant RLC circuits. By designing each target coil and capacitor to have a different resonant frequency, frequency selectivity can be achieved. An experimental system consisting of three resonant targets was built and tested. When compared to nonresonant frequency selectable induction heating targets, resonant RLC circuits have the potential for considerably higher preferential heating in a smaller frequency band. Care must be taken to insure that the network is sufficiently resonant and that the majority of losses are not associated

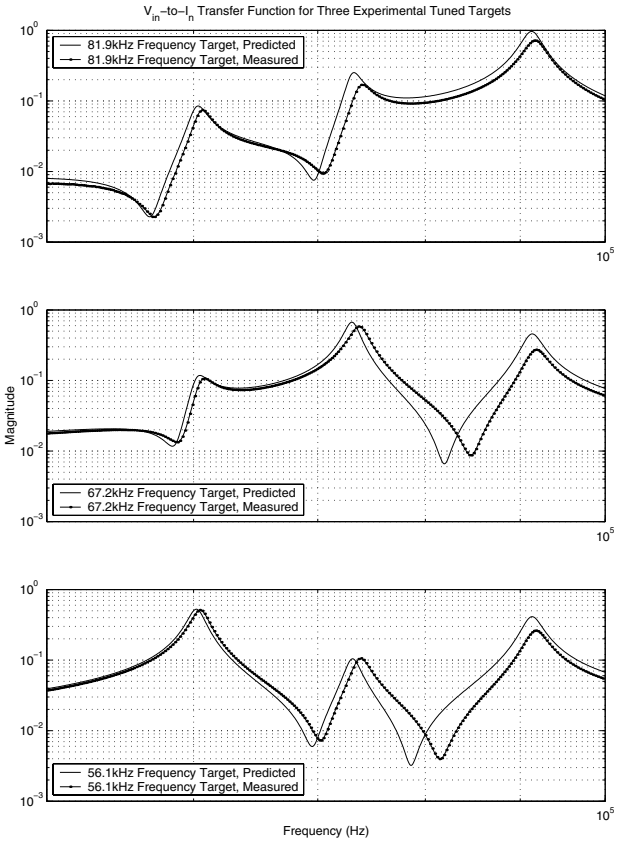

Fig. 12. Results of multi-resonant induction heating experiment.

with the resonant capacitor. One application of these targets is a tunable vibration damper we are developing. The damper relies on the fact that a rotating container filled with a variable viscosity material can alter its moment of inertia. In this case the rotating container consists of a set of individual compartments filled with a thermally responsive gel. Thermal stimulation of the different compartments allows the damper to adjust the location of its anti-resonant frequency. One way to thermally activate these compartments is by outfitting each chamber with a frequency selectable induction target. Any combination of chambers can then be simultaneously heated by the primary induction coil if it is driven at the appropriate frequencies with a voltage sum-of-sinewaves.

This multi-frequency, multi-target approach can be used in a wide range of applications, including medical and industrial processes, to provide a wide range of spatial temperature control. One such application is the treatment of deep-seated tumors using hyperthermia [11]-[14]. Currently, the generation of a desired spatial temperature gradient requires a complicated distribution of identical induction targets. The availability of frequency selectable targets would allow greater flexibility in the distribution of targets, especially, because the temperature profile can now be modified post target distribution simply by controlling the drive voltage across the primary induction coil.

Acknowledgements

The authors gratefully acknowledge the support of the National Science Foundation through a MRSEC grant to MIT's Center for Materials Science and Engineering, a grant from the Grainger Foundation, and support from the Ford Motor Company.

References

[1] Harris C., Crede C.,"Shock and Vibration Handbook (vol.1), McGrawHill, New York, 1961.

[2] Christopher Ting-Kong, "Design of an Adaptive Dynamic Vibration Absorber," *M.eng. Thesis,* Department of Mechanical Engineering, The University of Adelaide, South Australia 5005, April 1999.

[3] T. Tanaka, "Gels," Scientific American, vol. 244, no. 1, pp. 124-138, Jan. 1981

[4] Jackson, D.K.; Leeb, S.B.; Mitwalli, A.H.; Narvaez, P.; Fusco, D.; Lupton, E.C., Jr.; "Power electronic drives for magnetically triggered gels," Industrial Electronics, IEEE Transactions on , Volume: 44 Issue: 2 , Apr 1997 Page(s): 217 -225

[5] F. Forest, E. Laboure, F. Costa, J.Y. Gaspard, "Principle of a multi-load/single converter system for low power induction heating," IEEE Trans. Power Electronics, vol.15, no. 2, pp. 223-230, March 2000.

[6] J.I. Rodriguez and S.B. Leeb, "A Multilevel Inverter Topology for Inductive Power Transfer," Applied Power Electronics Conference, 2003. APEC '03. Eighteenth Annual, pp 1118-1126.

[7] J.I. Rodriguez, R. He, and S. Leeb, "Frequency selectable induction heating targets," Power Electronics Specialists Conference, 2003. PESC '03 34th Annual, pp 1943-1950.

[8] J. I. Rodriguez, "A Multi-Frequency Induction Heating System for a Thermally Triggered Gel Polymer Dynamic Vibration Absorber," *Ph.D. Thesis,* Massachusetts Institute of Technology, Expected June, 2003.

[9] H. A. Haus, and J. R. Melcher, *Electromagnetic Fields and Energy*, Prentice-Hall, 1989 ,pp. 446-447.

[10] Kamon, M.; Ttsuk, M.J.; White, J.K. "FASTHENRY:a multipole-accelerated 3-D inductance extraction program," Microwave Theory and Techniques, IEEE Transactions on , Volume: 42 Issue: 9 Part: 1-2 , Sept. 1994 Page(s): 1750 -1758

[11] P.I.Stauffer, T.C. Cetas, A.M. Fletcher, D.W. DeYoung, M.W. Dewhirst, J.R. Oleson, R.B. Roemer, "Observations on the user of Ferromagnetic Implants for inducing Hyperthermia," Biomedical Engineering, IEEE Transactions on, Volume: BME31, no. 1, Feb 1984, pp.76-90

[12] P.I.Stauffer, T.C. Cetas, R.C. Jones, "Magnetic Induction Heating of Ferromagnetic Implants for Inducing Localized Hyperthermia in Deep-Seated Tumors," Biomedical Engineering, IEEE Transactions on, Volume: BME31, no. 2, Feb 1984, pp.235-251

[13] A.Y. Matloubieh, R.B. Roemer, T.C. Cetas, "Numerical Simulation of Magnetic Induction Heating of Tumors with Ferromagnetic Seed Implants," Biomedical Engineering, IEEE Transactions on, Volume: BME31, no. 2, Feb 1984, pp.227-234

[14] Kimura, I.; Katsuki, T.; "VLF induction heating for clinical hyperthermia,"' Magnetics, IEEE Transactions on , Volume: 22 Issue: 6 , Nov 1986 Page(s): 1897 -1900

[15] J.S. Lai and F.Z. Peng, "Multilevel Converters–A New Breed of Power Converters," IEEE Trans. Ind. Applicat., vol. 32, no. 3, pp. 509-517, May/June 1996.